

Interpretation of the Mössbauer Spectroscopy Data by the Maximum Entropy Method

L. Dobrzyński*, A. Holas[†] and D. Satuła and K. Szymański**

**Institute of Experimental Physics, University of Białystok, 41 Lipowa, 15-424 Białystok, Poland
The Sołtan Institute for Nuclear Studies, 05-400 Otwock-Świerk, Poland*

*†Institute of Physical Chemistry of the Polish Academy of Sciences, 44/52 Kasprzaka, 01-224
Warsaw, Poland*

***Institute of Experimental Physics, University of Białystok, 41 Lipowa, 15-424 Białystok, Poland*

Abstract. A reconstruction of the 3-dimensional distributions of the magnetic hyperfine field, quadrupole splitting and isomer shift from the measured 1-dimensional Mössbauer spectrum is extremely difficult in general case. The paper shows that reliable reconstruction can be made by means of the Maximum Entropy Method without prior assumptions concerning correlations between the parameters of interest. We also show how the prior should be chosen in order to arrive at the physically meaningful results.

Key Words: Bayesian logic, Maximum Entropy Method, Mössbauer spectra

1. INTRODUCTION

The Maximum Entropy Method (MEM) [1] was already used to analyze many spectroscopic data [2, 3, 4, 5]. This powerful method was not extensively applied to the analysis of the Mössbauer spectra where presence of the distribution of hyperfine field parameters makes the spectra complicated and the spectra interpretation becomes ambiguous because of assumptions one makes in order to get the hyperfine field distributions. The one dimensional Mössbauer spectrum contains information on the distribution of the hyperfine magnetic field (B), quadrupole splitting (QS) and the isomer shift (IS), not speaking about orientations of the hyperfine magnetic fields, which cause often a lot of problems in some experiments. We checked recently [6] that rather complicated 2-dimensional distributions in (B, IS) space can be reconstructed from the Mössbauer spectra by MEM technique. This paper deals with more difficult cases. In spite of the fact that the 3-dimensional reconstruction of (B, QS, IS) distribution from a single spectrum seems almost impossible, a well-known inherent ambiguity problem [7, 8] consisting in the fact that many distributions of the hyperfine field can fit well to the experimental spectrum, makes the situation even worse.

In short, when the Zeeman interaction is dominating, the Mössbauer spectrum consists of lines measured as a function of the source velocity $V(k)$, where $k = 1, 2, \dots, N$ with N being usually 256. In typical experiment with ^{57}Fe -based absorption, for given hyperfine magnetic field B (in Tesla), isomer shift IS (in mm/s) and quadrupole splitting QS (in

mm/s), the recoilless absorption occurs at six velocities $\{v_i\}$ (Zeeman's sextet) linearly dependent on B , QS and IS , see, e.g., [6, 7, 8, 9]. In the case of infinitely thin absorber, the line intensities I_i should be as 3:2:1:1:2:3. More general formulas are given in ref. [9].

A given i th line contributes to the k th channel in the velocity spectrum the intensity proportional to

$$J_k = \frac{I_i}{(V(k) - v_i)^2 + (\Gamma/2)^2}, \quad (1)$$

where the natural width, Γ , of the line from Mössbauer source is 0.22–0.25 mm/s (in our calculations 0.24 mm/s was chosen). When the electric field gradient accompanies low magnetic hyperfine field, eight instead of six lines appear in the spectrum. The intensities have to be calculated from the solution of the so-called full Hamiltonian. In order not to complicate further considerations we shall not deal with this kind of complication, neither with another one consisting in the spectra distortions due to the finite thickness of an absorber or its possible magnetic texture.

There exist methods of reconstructing the hyperfine magnetic field distribution [10, 11, 12, 13, 14, 15, 16] from measured spectra. However, in order to make such reconstruction, one has usually to assume certain correlation between the parameters B , IS , and QS . To the best of the authors knowledge, there is no code enabling one to get, e.g., the distributions of B and IS independently of each other. Our earlier paper [6] showed that this can be done when the analysis is carried out by means of the Maximum Entropy Method. The first successful attempt to use this method for a single parameter distribution was published by Brand and Le Caër [17]. Dou et al. [18] used Bayesian inference theory to obtain the distribution of one parameter B assuming however a linear coupling of two other parameters (IS and QS) to B .

2. MAXIMUM ENTROPY METHOD

Assume that the whole 3-dimensional space of parameters was divided into pixels and the value ρ_j denotes the probability of having the values of these parameters corresponding to this particular pixel. Because the line intensities are linear in the probabilities, the intensities W_k measured (with uncertainties σ_k) at k th velocity channel will be described theoretically by:

$$T_k = \sum_{j=1}^{N_{pix}} r_{kj} \rho_j, \quad \text{where } k = 1, 2, \dots, N. \quad (2)$$

The transformation matrix $\{r_{kj}\}$ can easily be evaluated (see references given in the Introduction). We consider the distribution $\rho_j = \rho_{B, QS, IS}$, which means that the index j denotes a collection of the three indices corresponding to the variables B , QS and IS , respectively. In other words three-dimensional matrix $\{\rho_j\}$ of the probability distribution is written in eqs. (2) and (4) as a single row.

As usual one is maximizing the Lagrangian [19]:

$$L = \alpha S - \frac{1}{2} \chi^2 \quad (3)$$

under an additional constraint of normalization of the distribution $\{\rho_j\}$. In eq. (3)

$$S = - \sum_{j=1}^{N_{pix}} \rho_j \ln(\rho_j / \rho_{0j}) \quad (4)$$

and

$$\chi^2 = \sum_k \frac{1}{\sigma_k^2} (W_k - T_k)^2. \quad (5)$$

In eq. (4), ρ_{0j} denotes a prior (a model). The final equations to solve are of usual type

$$\rho_j = \frac{\rho_{0j} \exp\left(-\frac{1}{2\alpha} \frac{\partial \chi^2}{\partial \rho_j}\right)}{\sum_{j'=1}^{N_{pix}} \rho_{0j'} \exp\left(-\frac{1}{2\alpha} \frac{\partial \chi^2}{\partial \rho_{j'}}\right)}, \quad j = 1, 2, \dots, N_{pix}. \quad (6)$$

During calculations special care is taken to ensure the equality of the sum of measured intensities W_k and the sum of intensities T_k as calculated from eq. (2) for the distribution $\{\rho_j\}$.

3. AMBIGUITY PROBLEM IN THE CASE OF PARAMAGNETIC SPECTRA

Initially, the first goal of the analysis was to study the distribution of (QS, IS) parameters in UFe_5Sn , for which the Mössbauer spectrum was measured in paramagnetic phase [20], in which $B = 0$. In the experiment [19] well defined two quadrupole doublets were found, and from the conventional approach to the Mössbauer spectra analysis the situation looked simple and clear. The intensity ratio, appr. 4:1, of the doublets was as expected on the basis of the iron distribution among different crystallographic sites. However, the distribution obtained by MEM was unexpectedly much richer, so we decided to study the situation of simulated two doublets: $(QS, IS) = (0.287, -0.064)$ and $(0.235, 0.115)$ (all parameters are expressed in mm/s and are close to the ones found in [19]). Fig. 1A presents the simulated spectrum consisting of these doublets. The Maximum Entropy Method with the uniform prior gave again very rich landscape of $P(QS, IS)$, see Fig. 1B, almost identical with the one obtained from the experimental spectrum. It could thus seem at first that MEM produces simply wrong answers. This, however is not the case. In fact, one can easily calculate that the landscape seen in Fig. 1B shows all possible combinations of doublets and singlets which could explain the measured spectrum, and satisfy the condition of the maximum of the entropy S . The symmetry with respect to the change of the sign of QS derives simply from the absorption cross section.

Obviously, the aforementioned solution consisting of the two doublets only is hidden among other possibilities considered by MEM. In order to get unique solution within the framework of MEM one thus has either to know some physical constraints or try some tricks. In the particular case considered by us we see that the first doublet is seen in Fig.

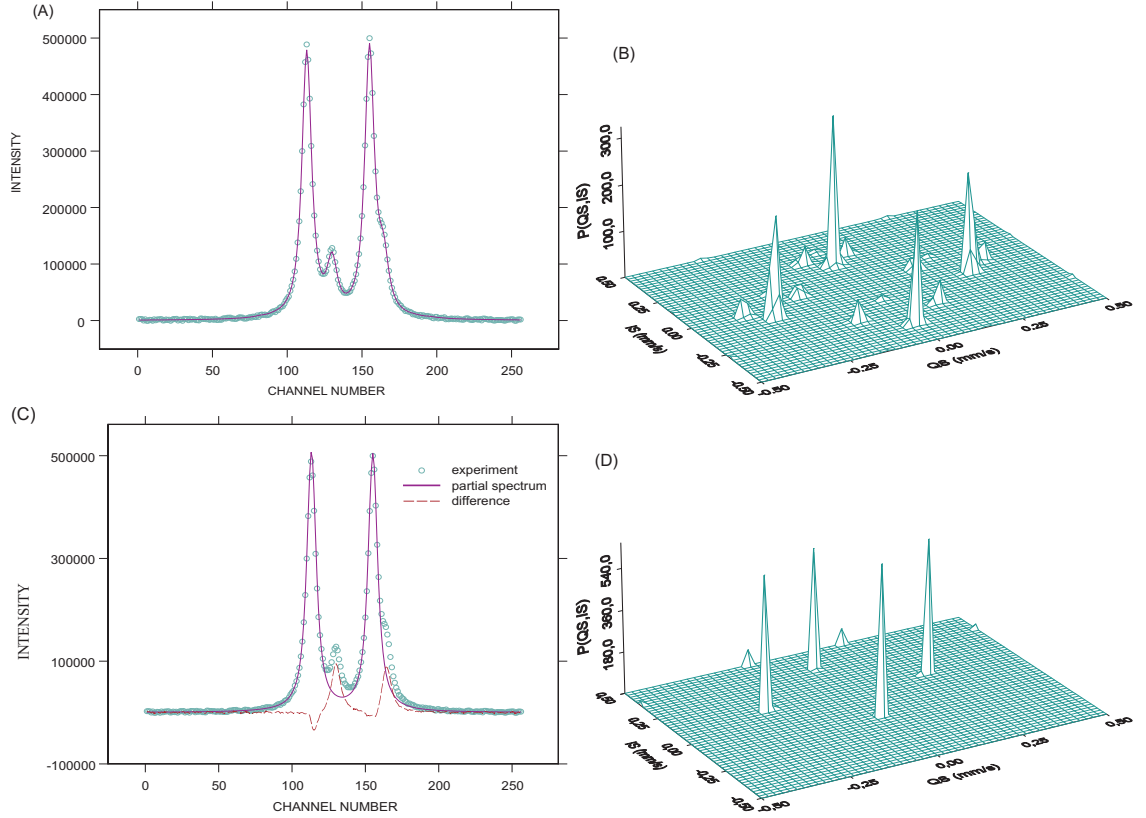


FIGURE 1. Simulated Mössbauer spectrum close to the experimentally observed for UFe_5Sn at room temperature [19]. (A) simulated (points) and reconstructed (solid line) spectrum; (B) reconstruction using uniform prior; (C) the spectrum corresponding to the strongest peak (solid line) and the difference spectrum (dashed line); (D) reconstruction from the difference spectrum.

1B with the highest intensity, i.e. it is found to be most likely. Therefore one can use it for calculating the Mössbauer spectrum which would result for this doublet only, and find its intensity so to get the best agreement with the measured spectrum in the sense of the least-square method. Next this partial spectrum can be subtracted from the total one, so the difference spectrum shown in Fig. 1C is obtained. There is a small narrow negative dip in the difference spectrum which shows that the line position or/and shape was not fitted precisely. This however, may well be due to the grid used and does not affect the final result. The MEM analysis of the difference spectrum leaves no doubts that in the total spectrum there is no more than another doublet, see Fig. 1D, in full agreement with what would be obtained from conventional analysis of the Mössbauer data. What we see in the Fig. 1D is equivalence of the doublet to two Lorentzian lines at $QS = 0$, and symmetric solution with respect to the $QS = 0$ axis. One can also note small noise in the reconstructed spectrum at the border of the range in which the reconstruction took place. This may arise from the uncertainties in the difference spectrum used for analysis and will have no physical meaning anyway.

The ambiguity problem is well-known and, as shown e.g. in ref. [13], when there is more than a single distribution of hyperfine field parameters in the paramagnetic phase,

the infinite number of distributions can be produced, all of which will be in perfect agreement with the measured Mössbauer spectrum. The Maximum Entropy Method is just giving its natural constraint which helps to find the most likely distribution. However, on the example presented above one can see that in addition to the MEM constraint which selects mathematically plausible result, one has to consider physical implications of the obtained distributions and seek eventually for the distributions with least number of features.

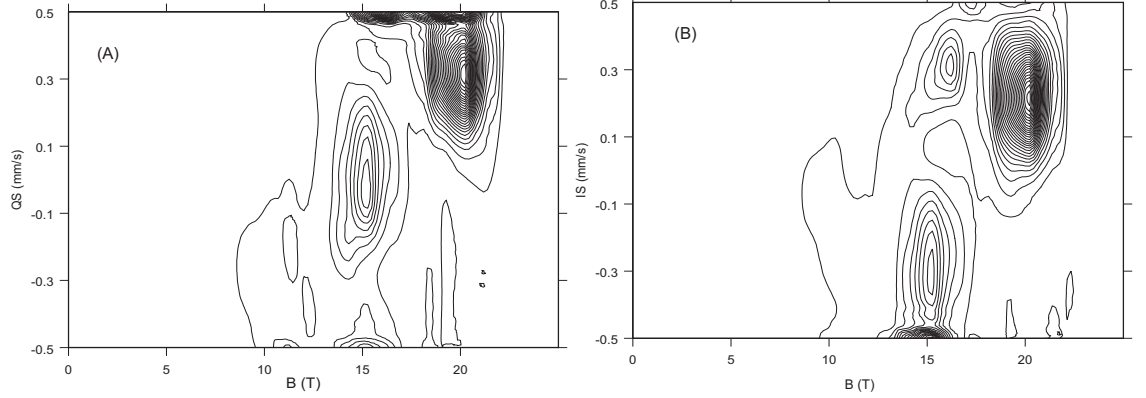


FIGURE 2. Distributions obtained with the uniform prior: (A) the marginal $P(B, QS)$; (B) the marginal $P(B, IS)$.

4. THREE-DIMENSIONAL PROBABILITY DISTRIBUTIONS

The feasibility of MEM in the case of 3-dimensional distribution was checked on the following simulated distribution:

$$\begin{aligned}
 P(B, QS, IS) = & \exp\left(-\frac{(B-20)^2}{4} - \frac{(QS-0.3)^2}{0.01} - \frac{(IS-0.2)^2}{0.01}\right) \\
 & + 0.5 \exp\left(-\frac{(B-15)^2}{4} - \frac{(QS-0.1)^2}{0.01} - \frac{(IS+0.2)^2}{0.01}\right) \\
 & + 0.25 \exp\left(-\frac{(B-10)^2}{4} - \frac{(QS+0.1)^2}{0.01} - \frac{IS^2}{0.01}\right). \quad (7)
 \end{aligned}$$

Here B is expressed in Tesla, while QS and IS in mm/s. Normalization constant is neglected as irrelevant parameter for our purpose. The calculated Mössbauer spectrum corresponding to this distribution is shown by points in Fig. 3A (the remaining content of Fig. 3 will be discussed later on). We find that the simulated distribution (7) is reconstructed perfectly if this distribution is used as a prior, so the MEM itself does not produce any substantial noise. On the other hand, although the Mössbauer spectrum is still reproduced very well, the reconstruction is rather poor if uniform prior is used. Therefore various non-uniform priors have been tried. Such priors are easily guessed if one has some experience with the Mössbauer spectra. We also noted that even in the case of poor reconstruction, the marginal probabilities [e.g., $P(B, QS) = \int P(B, QS, IS) dIS$]

are reproduced very well, and show peaks at $B = 10, 15$ and 20 , so the marginal $P(B)$ can always be used as a prior. In addition, even from the results obtained with uniform prior, see Fig. 2, one can postulate appearance of the strongest peak at $B = 20$, $QS = 0.3$ and $IS = 0.2$, and thus use the following prior

$$P(B, QS, IS) = \exp\left(-\frac{(B-20)^2}{4} - \frac{(QS-0.3)^2}{0.01} - \frac{(IS-0.2)^2}{0.01}\right) + 0.5 \left[\exp\left(-\frac{(B-15)^2}{4}\right) + \exp\left(-\frac{(B-10)^2}{4}\right) \right] \exp\left(-\frac{QS^2}{0.02} - \frac{IS^2}{0.02}\right). \quad (8)$$

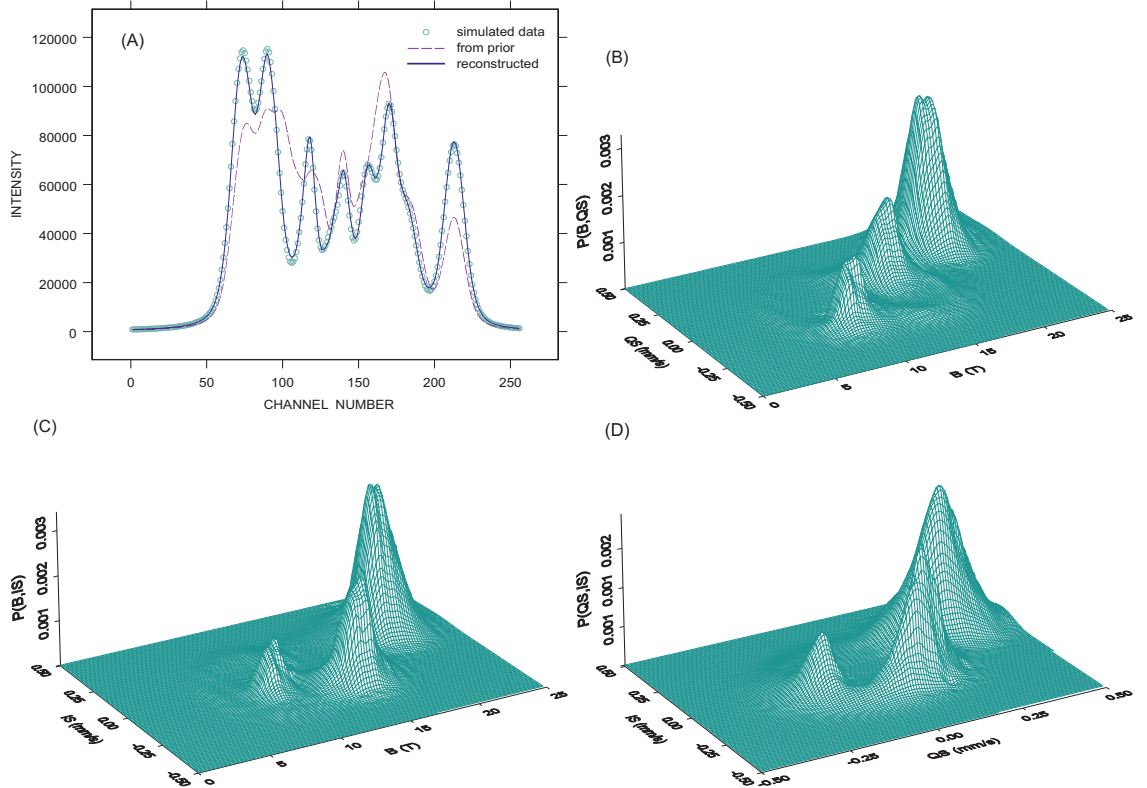


FIGURE 3. (A) The pseudo-experimental spectrum and the fitted one (solid line) with the prior as given in eq. (8). The spectrum corresponding to this prior is shown by dashed line; (B) marginal $P(B, QS)$ reconstructed from the prior (8); (c) same for $P(B, IS)$; (d) same for $P(QS, IS)$. All probabilities given in arbitrary units.

Note that although in $P(B)$ the intensities of two peaks found at $B = 15$ and $B = 10$ were apparently different, we used in (8) the same amplitude for both of them, while leaving rather large uncertainty concerning respective values of QS and IS . The spectrum corresponding to this prior (note that it is quite different from the “measured” one) and the results of the final reconstruction presented in 3-dimensional graphs are shown in Figs. 3A–D. There is no doubt that in spite of some small artefacts the reconstruction was successful. The similarity of Figs. 3C and 3D is not strange as the formula (7) indicates linear correlation of B and QS . However, this correlation had to be found by MEM!

5. CONCLUSIONS

It was shown that the reconstruction of the probability distribution of the hyperfine parameters from Mössbauer spectrum is possible, although one has to be very careful with coming to conclusions. We have shown that the Maximum Entropy Method gives the most likely distribution which, however, can have little to do with the true one. Therefore some extra work is needed for interpreting the spectrum. This does not show any weakness of the MEM method. Just the opposite is true. One should remember that all conventional methods of analysis rely on assumptions of e.g. the number of subspectra and possible correlations between hyperfine parameters. Therefore, a true advantage of MEM consists in abandoning the latter assumptions. As we showed, the MEM can successfully be applied to reconstruction of even 3-dimensional distributions from the one-dimensional Mössbauer spectra, provided, however, that a proper non-uniform prior is used.

REFERENCES

1. E. T. Jaynes, *Probability Theory. The Logic of Science*, Cambridge: Cambridge University Press, (2003).
2. G. L. Bretthorst, *Bayesian Spectrum Analysis and Parameter Estimation*, Lecture Notes in Statistics 48, Berlin: Springer-Verlag, (1988).
3. *Maximum Entropy in Action*, edited by B. Buck and V. A. Macaulay, Oxford: Clarendon Press (1991).
4. U. Gerhard, S. Marquardt, N. Schroeder, S. Weiss, Bayesian deconvolution and analysis of photoelectron or any other spectra: Fermi-liquid versus marginal Fermi-liquid behavior of the 3d electrons in Ni, *Phys. Rev. B* **58**, 6877 (1998).
5. L. Dobrzyński, "Momentum Density Studies by the Maximum Entropy Method" in *X-Ray Compton Scattering*, edited by M. J. Cooper et al., Oxford: Oxford University Press (2004), pp.188–209.
6. L. Dobrzyński, K. Szymański, D. Satuła, *Nukleonika* **49**, Suppl. 3, S89 (2004).
7. G. Le Caër, J. M. Dubois, H. Fischer, I. U. Gonser, H. G. Wagner, *Nucl. Instr. Meth.* **B5** 25 (1984).
8. G. Le Caër, R. A. Brand, General methods for the distributions of electric field gradients in disordered solids. *J. Phys.: Condens. Matter* **10**, 10715–10774 (1998).
9. K. Szymański, L. Dobrzyński, D. Satuła and B. Kalska-Szostko "Trends in Mössbauer polarimetry with circularly polarised radiation" in *Material Research in Atomic Scale by Mössbauer Spectroscopy*, edited by M. Mashlan, M. Miglierini and P. Schaaf, Nato Science Series, II Mathematics, Physics and Chemistry, Vol 94, Dordrecht: Kluwer Academic Publishers, 2003, pp. 317–328.
10. F. Varret, A. Gerard, P. Imbert, Magnetic field distribution analysis of the broadened Mössbauer spectra of zinc ferrite, *Physica Status Solidi B — Basic Research*, **43**, 723 (1971).
11. B. Window, Hyperfine field distributions from Mössbauer spectra, *J. Phys. E: Scientific Instruments*, **4**, 401 (1971).
12. T. E. Cranshaw, The deduction of the best values of the parameters from Mössbauer spectra, *J. Phys. E: Scientific Instruments*, **7**, 122-124 (1974).
13. G. Le Caër, J. M. Dubois, Evaluation of hyperfine parameter distributions from overlapped Mössbauer spectra of amorphous alloys, *J. Phys. E: Scientific Instruments*, **12**, 1083–1090 (1979).
14. S. J. Campbell, G. J. Whittle, A. M. Stewart, On the determination of the magnetic hyperfine field distribution in an amorphous alloy, *Journal of Magnetism and Magnetic Materials*, **31–34**, 1521–1522 (1983).
15. J. Hesse, A. Rubartsch, Model independent evaluation of overlapped Mössbauer spectra, *J. Phys. E: Scientific Instruments*, **7**, 526–532 (1974).
16. M. A. Chuev, O. Hupe, H. Bremers, J. Hesse, A. M. Afanas'ev, A novel method for evaluation of complex Mössbauer spectra demonstrated on nanostructured ferromagnetic FeCuNiB alloys, *Hyperfine Interactions*, **126**, 407–410 (2000).

17. R. A. Brand, G. Le Caër, Improving the validity of Mössbauer hyperfine parameter distributions: the maximum entropy formalism and its applications, *Nuclear Instruments and Methods*, **B34**, 272–284 (1988).
18. L. Dou, R. J. W. Hodgson, D. G. Rancourt, Bayesian inference theory applied to hyperfine parameter distribution extraction in Mössbauer spectroscopy, *Nuclear Instruments and Methods*, **B100**, 511 (1995).
19. J. Skilling, W. Bryan, *Mon. Not. T. Astr. Soc.*, **211**, 111-124 (1984).
20. D. Satuła, K. Szymański, V. H. Tran, L. Dobrzyński, *Nukleonika* (to be published).